Crystal Engineering Involving C−H···N Weak Hydrogen Bonds: Penannular Enclosure of Organic Guests by a Diquinoline Host

A. Noman M. M. Rahman,[a] Roger Bishop,*[a] Donald C. Craig,[a] and Marcia L. Scudder[a]

Keywords: Crystal engineering / Host-guest systems / Hydrogen bonds / Crystal structures

The preparation and properties of the racemic lattice inclusion host 6α,13α-dibromo-5bα,6,12bα,13-tetrahydropentaleno[1,2-*b*:4,5-*b*′]diquinoline (**8**) are described. Strong hydrogen bonding interactions are not possible for this versatile host compound. Instead, weaker interactions (such as aryl offset face-face, aryl edge-face, halogen-halogen, halogen-π, and C–H···N synthons) compete against each other to generate the inclusion structure of lowest energy. The guests are contained within molecular pens formed by two hosts enclosing each guest. These host molecules are not directly linked at the corners of the pen, but rather assemble with their neighbours into layers of pens by means of aryl offset face-face interactions. The C–H···N weak hydrogen bond plays a dominant role in these structures by linking adjacent layers edge-edge through two distinct types of double motifs. One is the previously recognised aryl C–H···N dimer, while the other is a new bifurcated Ar–H···N···H–CBr–Ar interaction. The X-ray structures of nine inclusion compounds formed by **8** are reported. Seven of these in space group $P2_1/c$ have isostructural host lattices where the layers of pens are stacked to produce guest channels. Several different guest arrangements are observed. In contrast, $(\mathbf{8})_2\cdot(CH_3CCl_3)$ in space group $C2/c$ and $(\mathbf{8})_2\cdot(CF_3C_6H_5)$ in $P2_12_12_1$ have the pen layers stacked so as to enclose their guests in cages. The structure of the nonbrominated precursor **7**, which undergoes self-resolution on crystallisation, is also described in crystal engineering terms.

Introduction

Lattice inclusion (clathrate) compounds are materials where one type of molecule (the guest) is trapped within the lattice of a second molecular type (the host).[1] The stability of these novel materials arises from the multiplicity of weak host-guest interactions constituting the overall crystal lattice, but this characteristic also makes their structures and properties difficult to predict. A major aim of contemporary solid-state chemistry is, therefore, to develop a true understanding of these substances.[2] Since supramolecular chemistry may be described[3] as "the designed chemistry of the intermolecular bond" our rapidly advancing knowledge of noncovalent interactions,[4] supramolecular synthons,[5] and crystal engineering[6] may be used to assist developing new clathrate systems in a logical manner.

Recently we have adopted a general approach for the synthesis of new families of lattice inclusion compounds based on the host structure illustrated in Figure 1. Planar aromatic wings are fused to a flexible central alicyclic linker group that imposes C_2 symmetry on the molecule. The *exo* sensor groups provide intermolecular contacts for either hosts or guests, while at the same time ensuring that the host molecules pack less efficiently with themselves. Thus, guest inclusion is encouraged by the structural nature of the dihalo compounds **1**−**3**, whereas the unsubstituted diquinoline **4** is not a host compound. Furthermore, in the synthesis of such hosts, the three modular construction units may be replaced by alternatives without sacrificing the lattice inclusion properties.

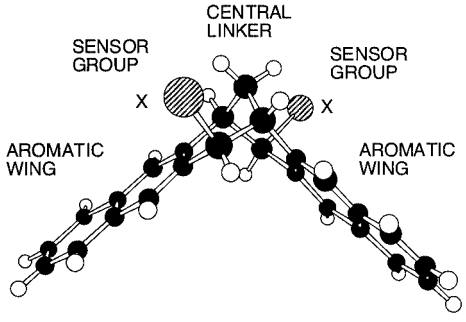

Figure 1. General design for obtaining new lattice inclusion hosts, such as compounds **1**−**3**, based on a modular synthetic approach

This approach is proving to be highly successful in producing new host systems. For example, variation of the aromatic wings or sensor groups has allowed us to prepare the new host molecules **1**−**3** all of which have a preference for

[a] School of Chemical Sciences, The University of New South Wales,
UNSW Sydney NSW 2052, Australia
Fax: (internat.) + 61-2/9385-6141
E-Mail: r.bishop@unsw.edu.au

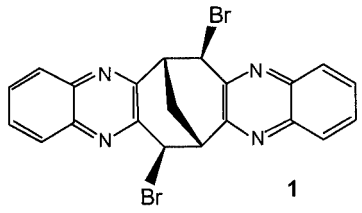

1

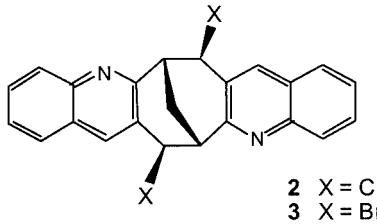

2 X = Cl
3 X = Br
4 X = H

trapping small polyhalogen compounds. The diquinoxaline host **1**[7] forms layer, tube, and cage structures when it combines with its guests, while the diquinolines **2** and **3** form layer and tube structures.[8,9]

Strong hydrogen bonding interactions are usually not observed for host compounds of the type **1**−**3**. Instead, weaker interactions (such as aryl offset face-face, aryl edge-face, halogen-halogen, halogen-π, and C−H···N synthons) compete against each other reversibly, ultimately furnishing the combination that affords the inclusion structure of lowest energy. The conformational flexibility[10] of the central linker unit provides a further means of optimising the host-guest packing in each specific case.

This approach has some parallels with the dynamic combinatorial chemistry used by Sanders to allow a molecule of interest to choose its optimum receptor from a complex molecular mixture.[11] For some host systems, such as our helical tubuland diols, the hydrogen bonding network dominates to such an extent that accurate prediction of inclusion structures can be made.[12] In the present case, however, we have host and guest molecules that can explore reversibly many potential assembly arrangements before reaching their optimum lattice inclusion structure. It therefore follows that for lattice inclusion systems involving a mixture of weak and reversible interactions the prediction of detailed structural outcomes will become more difficult.

The above hosts and their inclusion compounds provide excellent probes for investigation of the weaker supramolecular synthons and their interrelationships. In particular, they allow study of the C−H···N interaction[13] in a systematic manner.[7] This is significant because the roles and applications of this weak hydrogen bond in crystal engineering[14] have been overshadowed so far by the more comprehensive studies of its C−H···O cousin.[15]

Results and Discussion

Preparation of the Inclusion Host 8

In the present work we have retained the dibromo sensor groups of the hosts **1**, **3** and the diquinoline wings used in structures **2**, **3**. The central linker group, however, has been changed from bicyclo[3.3.1]nonane to the bicyclo[3.3.0]octane moiety. This minor alteration in molecular structure − simple removal of a CH_2 unit − results in deep-seated changes to the resulting inclusion structures.

The synthesis of the new diquinoline host **8** is shown in Scheme 1; 2 equiv. of 2-aminobenzaldehyde (**5**)[16] were condensed with 1 equiv. of racemic bicyclo[3.3.0]octane-2,6-dione (**6**)[17] by means of a Friedländer reaction[18] to yield the diquinoline adduct **7** in 75% yield. As found earlier for the preparations of **1** and **3**, free radical bromination using *N*-bromosuccinimide (NBS) proceeds with regio- and stereoselectivity and afforded the racemic target compound **8** in 78% yield.

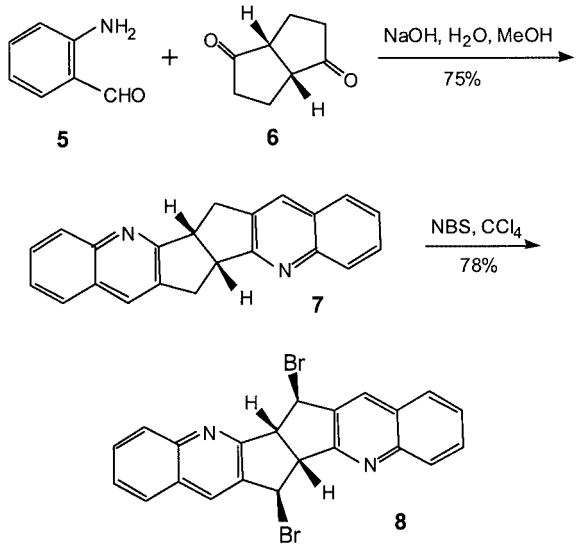

Scheme 1. Preparation of the bicyclo[3.3.0]octane-based diquinoline host **8**

Crystal Structure of Diquinoline 7

During our earlier studies on compounds **2**−**4** we had found that the parent nonhalogenated derivative **4** crystallised easily as a racemic guest-free structure as, indeed, had been expected. Its X-ray structure showed that molecules of this diquinoline packed together efficiently in its crystal lattice.[9] It was therefore a surprise to find that it was very difficult to obtain crystalline samples of its bicyclo[3.3.0]octane analogue **7**. Crystals could be grown from ethanol as laths that were too thin for X-ray structure determination, but slightly thicker plates were obtained eventually from dioxane solution and these proved suitable. Numerical details of the solution and refinement of this analysis are presented in Table 1.

Diquinoline **7** crystallises as a conglomerate,[19] the racemic material having undergone self-resolution to yield a 1:1 mixture of (+)- and (−)-crystals.[20] This was a further surprise based on the previous behaviour of its analogue **4**. Resolved solid **7**, in chiral space group *C*2, has all its molecules in the same orientation and packed into parallel stacks. Effective aryl offset face-face (OFF) interactions[21] are present between the parallel aromatic wings within these stacks (Figure 2, part a). The view normal to this (Figure 2, part

Table 1. Numerical details of the solution and refinement of the crystal structures

	7	$(\mathbf{8})_2\cdot(CCl_3CH_3)$	$(\mathbf{8})_2\cdot(C_7H_5F_3)$	$(\mathbf{8})_2\cdot(C_4H_8O_2)$ (dioxane)	$(\mathbf{8})_2\cdot(C_4H_8O_2)$ (ethyl acetate)	$(\mathbf{8})_2\cdot(C_3H_6O)_{1.5}$	$(\mathbf{8})_2\cdot(C_4H_5N)\cdot(C_2H_3N)_{0.5}$
Formula of asymm. unit	$(C_{22}H_{16}N_2)_{0.5}$	$C_{22}H_{14}Br_2N_2$, $(C_2H_3Cl_3)_{0.5}$	$(C_{22}H_{14}Br_2N_2)_2$, $C_7H_5F_3$	$(C_{22}H_{14}Br_2N_2)_2$, $C_4H_8O_2$	$(C_{22}H_{14}Br_2N_2)_2$, $C_4H_8O_2$	$(C_{22}H_{14}Br_2N_2)_2$, $(C_3H_6O)_{1.5}$	$(C_{22}H_{14}Br_2N_2)_2$,C_4H_5N, $(C_2H_3N)_{0.5}$
M	154.2	532.9	1078.5	1020.5	1020.5	1019.5	1020.0
Crystal system	monoclinic	monoclinic	orthorhombic	monoclinic	monoclinic	monoclinic	monoclinic
Space group	*C*2	*C*2/*c*	$P2_12_12_1$	$P2_1/c$	$P2_1/c$	$P2_1/c$	$P2_1/c$
a [Å]	12.625(6)	17.006(9)	13.800(3)	14.763(5)	14.809(9)	14.909(6)	14.937(7)
b [Å]	4.659(1)	18.764(4)	16.213(6)	16.852(6)	16.658(9)	16.703(4)	16.831(3)
c [Å]	13.134(6)	13.421(7)	19.088(5)	18.023(7)	17.984(9)	18.078(8)	18.053(8)
β [°]	98.04(2)	92.05(3)	90	110.64(3)	110.58(5)	110.99(2)	111.19(2)
V [Å^3]	764.9(6)	4280(3)	4271(2)	4196(5)	4153(4)	4203(2)	4232(3)
D_c [g cm^{-3}]	1.34	1.65	1.68	1.62	1.63	1.61	1.60
Z	4	8	4	4	4	4	4
μM_o [mm^{-1}]	0.574[a]	3.950	3.785	3.841	3.881	3.834	3.807
$2\theta_{max.}$ [°]	140[a]	50	50	46	46	50	44
Crystal decay	9%	0%	5%	0%	0%	0%	0%
Min. trans. factor	–	0.40	0.38	0.42	0.45	0.48	0.37
Max. trans. factor	–	0.57	0.73	0.69	0.60	0.68	0.59
Unique refl.	843	3761	4173	5477	5752	7382	5169
Observed refl.	750	1612	1994	2601	2568	2954	2711
R_{merge}	0.007	0.056	–	0.019	0.045	0.028	0.017
R	0.059	0.061	0.057	0.042	0.095	0.050	0.051
R_w	0.085	0.077	0.059	0.048	0.115	0.057	0.061
CCDC-	-189724	-189725	-189726	-189727	-189728	-189729	-189730

[a] Copper radiation (λ = 1.5418 Å) was used for this structure.

b), down the stacks, shows the fair aryl edge-face (EF) interactions[21,22] that operate between the wings of adjacent stacks.

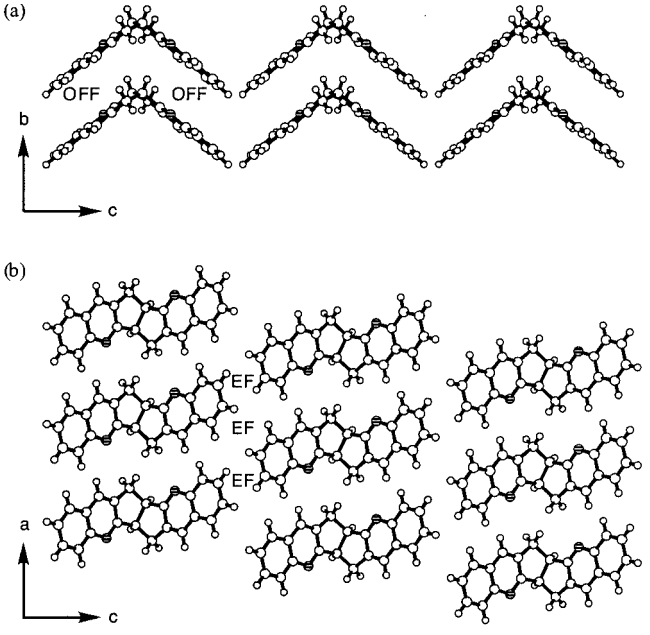

Figure 2. The molecules in crystalline chirally pure **7** are arranged as parallel stacks along *b*; (a) parts of three stacks showing the ideal packing for intrastack OFF interactions between the aromatic wings; the rows of stacks behind and in front of the one illustrated are identical, but are translated along *b* and situated midway between the molecules of **7** shown here; (b) a projection of nine stacks in the *ac* plane showing interstack association by means of EF interactions; nitrogen atoms are indicated by horizontal hatching

The other notable interaction is C−H···N weak hydrogen bonding which plays a major role in stabilising the crystal lattice.[13] Each quinoline nitrogen atom participates in a bifurcated interaction with two hydrogen atoms in different neighbouring molecules. This Ar−H···N···H−CH−Ar interaction involves an aromatic hydrogen atom (C−*H*···*N* 3.05 and *C*−H···*N* 3.99 Å), and also a benzylic methylene hydrogen atom (Ar−CH−*H*···*N* 2.89 Å and Ar−*C*H−H···*N* 3.71 Å), as illustrated in Figure 3. Repetition of this arrangement affords a network of C−H···N hydrogen bonds throughout the crystal.

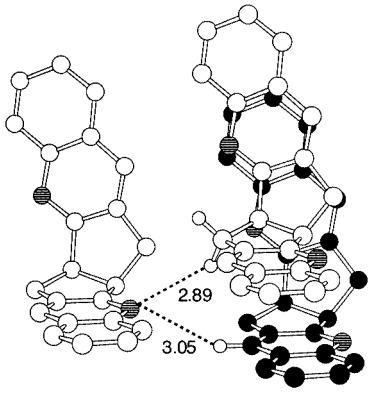

Figure 3. The bifurcated Ar−H···N···H−CH−Ar hydrogen bond motif involving three identical homochiral molecules of **7**; dashed lines indicate the C−*H*···*N* distances (3.05 and 2.89 Å); for clarity, hydrogen atoms other than those at the contact points are omitted, and the carbon atoms of one molecule of **7** are in black

Inclusion Compounds of the Host 8

Crystallisation of the dibromide **8** from many common solvents results in formation of lattice inclusion compounds. Crystals suitable for X-ray structure determination were obtained using 1,1,1-trichloroethane, α,α,α-trifluorotoluene, dioxane, 1,1,2,2-tetrachloroethane, chloroform, ethyl acetate, acetone, 1,2-dichlorofluoroethane, and allyl cyanide/acetonitrile. Numerical details of the solution and refinement of six key examples are presented in Table 1, and data for all nine have been deposited.[23]

All of these compounds have the same basic type of inclusion structure despite the variations in guest functionality. Their most obvious common feature is that two molecules of **8** surround one guest molecule forming a pen-annular assembly. If these host pairs were covalently bonded at the corners then the resulting structure would be a cyclophane,[24] but only marginal aromatic edge-face (EF) noncovalent contacts are present at these sites. This type of inclusion is entirely different to those observed for the hosts **1**−**3** that have a bicyclo[3.3.1]nonane central linker.[7−9] Furthermore, the structural consistency over the range of inclusion compounds contrasts with the highly variable behaviour noted for these earlier hosts.

A colourful, but rather useful, means of visualising the host-guest packing is the comparison with animals being held in the small enclosures of a stockyard. Each guest molecule represents a captive animal, and the four planar aromatic wings surrounding it are analogous to the fences of its enclosure. These molecular pens pack together in layers, assisted by aryl offset face-face (OFF) π-π attractions. Since host-host and host-guest forces are weak, these pens can adapt their dimensions and geometries to accommodate differently shaped guest molecules.

In all nine of the inclusion structures, adjacent layers of pens associate edge-edge by means of networks of dimeric C−H···N weak hydrogen bonds. Although this mode of assembly is less obvious at first sight, arguably it is the dominant intermolecular association in these structures.

Crystal Structure of $(8)_2\cdot(CH_3CCl_3)$

Crystallisation of racemic **8** from 1,1,1-trichloroethane (methylchloroform) yields crystals of $(8)_2\cdot(CH_3CCl_3)$ in space group *C*2/*c*. This structure is the simplest of the inclusion structures of **8**, presumably due to the guest being nearly spherical in shape. Only one molecule of **8** is present in the asymmetric unit, and only one type of pen with a nearly square cross-section is formed. Only poor EF interactions are present at the pen corners. The lattice involves layers of pens, where each pen contains one guest molecule. Aromatic OFF interactions[22] are prominent in the interpen assembly but there are no bromine-bromine[25] interactions under 4.0 Å within the layers. The plane of the pens contains parallel twofold and twofold screw axes. The twofold axes generate one side of the pen from the other, while the twofold screws relate adjacent pens within the layer (Figure 4, part a).

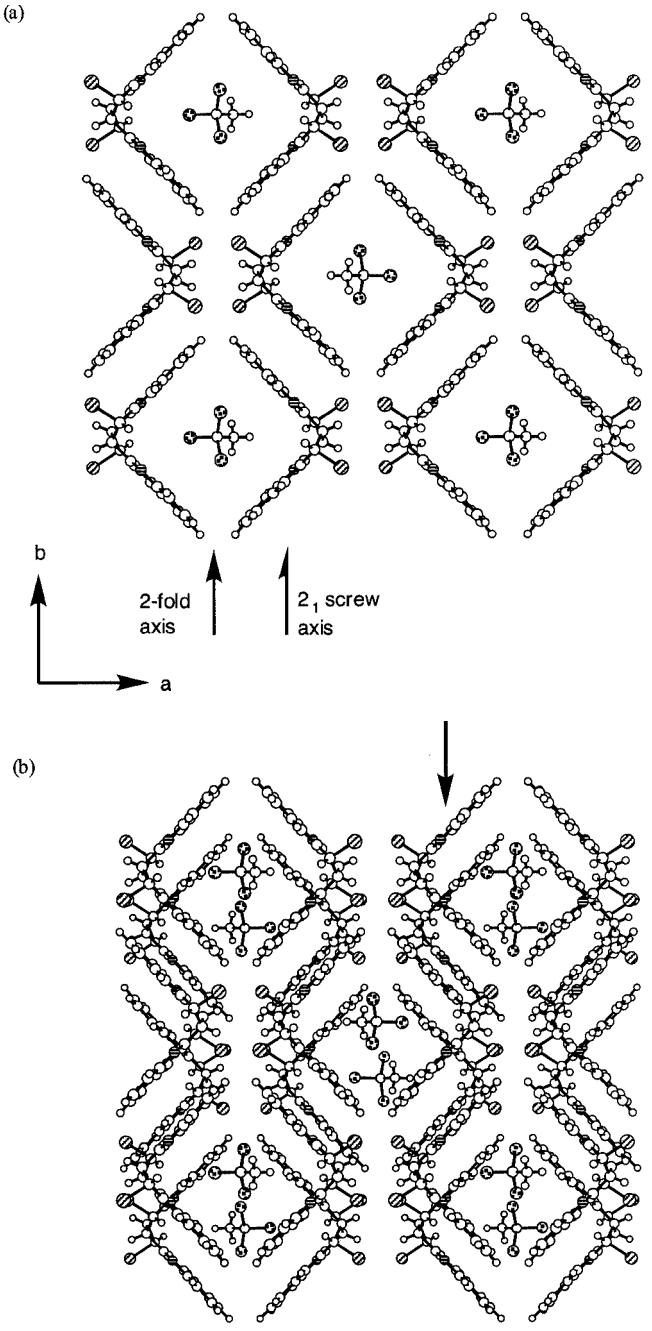

Figure 4. (a) Part of the structure of $(8)_2\cdot(CH_3CCl_3)$ showing a projection in the *ab* plane of one layer of molecular pens and their included guests; interpen OFF interactions are apparent; only one disorder component of the methylchloroform guest is shown for clarity; (b) a similar projection of two adjacent layers showing their offset stacking; the arrow marks the row of host molecules illustrated in Figure 5 (b); atom designators: N (horizontal hatching), Br (diagonal hatching), Cl (stippling)

The combination of twofold and twofold screw axis symmetry elements results in homochiral host layers. Two adjacent layers are related to the first by inversion which leads to them being composed entirely of host molecules of the opposite enantiomer. These layers of pens stack offset to each other so that the space above and below the guest is partially occupied by the adjacent layer. Hence the guest

molecules occupy individual cage-like voids within the lattice (Figure 4, part b). Because methylchloroform has nearly tetrahedral symmetry, the guest molecules are rotationally disordered within these cages.

The layers are linked by Br···Br interactions (3.69 Å) and a network of C−H···N weak hydrogen bonds. Two distinct double interlayer motifs occur for the latter as shown in Figure 5, part a. One of these is the familiar[9] edge-edge aryl C−H···N dimer that links opposite enantiomers of **8** in adjacent layers. As usual, this motif is centrosymmetric with both intermolecular distances identical (C−*H*···*N* 2.47 and *C*−H···*N* 3.38 Å).

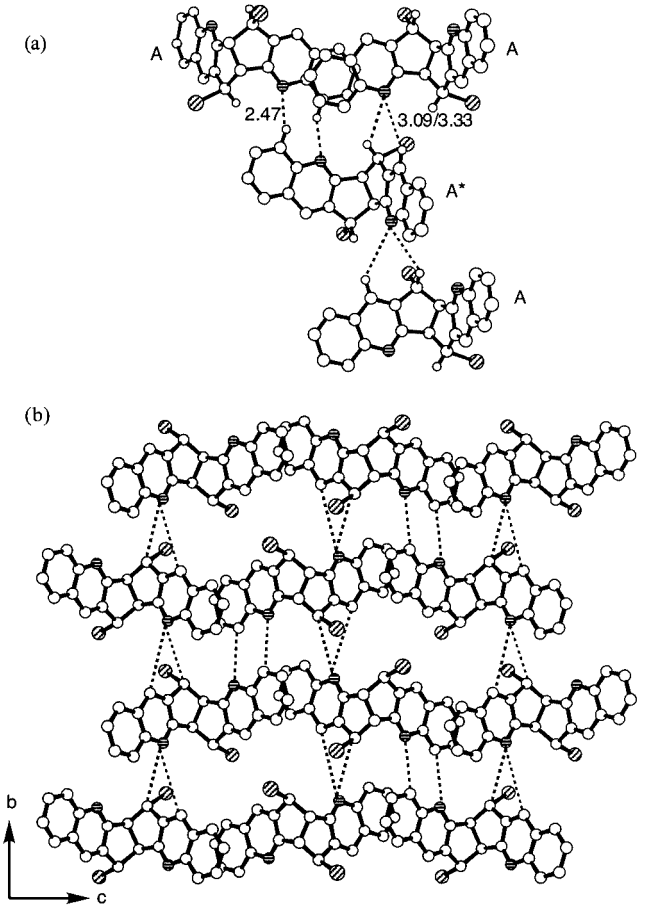

Figure 5. (a) The three interlayer double C−H···N weak hydrogen bonds (dashed lines) subtended by each host molecule in $(\mathbf{8})_2{\cdot}(CH_3CCl_3)$; one of these is a centrosymmetric edge-edge dimer, while the other two (one H-donor and one H-acceptor from the same aromatic wing) are identical examples of the new bifurcated interaction; for clarity, only the hydrogen atoms at the contact points are illustrated; (b) part of the network of multiple C−H···N interactions present in the lattice, obtained by repeating the above motifs between four host layers; here all hydrogen atoms are omitted for clarity

Recently we have described the aza-1,3-*peri* aromatic hydrogen interaction. This bifurcated C−H···N motif involves double interaction with two aromatic hydrogen atoms.[26] The second interaction between layers of **8** is related to this, but is a new variant. It occurs where two wing edges abut orthogonally. A quinoline nitrogen atom belonging to one layer interacts with two hydrogen atoms of a host molecule in the adjacent layer by means of a bifurcated Ar−H···N···H−CBr−Ar arrangement. Half of the motif still involves an aromatic hydrogen atom (C−*H*···*N* 3.33 and *C*−H···*N* 4.13 Å), but now the second half involves an aliphatic CHBr hydrogen atom (C−*H*···*N* 3.09 and *C*−H···*N* 3.78 Å).

The effectiveness of the interlayer C−H···N network can be gauged from Figure 5, part b. This is generated by taking four layers (analogous to the two layers shown in Figure 4, part b), selecting a band of molecules of **8** along the *b* axis (indicated by the arrow in Figure 4, part b) that comprises four chains of host molecules of **8** (with molecules in each chain linked through OFF interactions), and then rotating this band into the *bc* plane. The result reveals how repetition of the unit in Figure 5, part a, results in multiple C−H···N hydrogen bonding between layers of pens.

A comparison of the C−H···N interactions present in all nine inclusion compounds formed by **8** is presented in Table 2.

Crystal Structure of $(\mathbf{8})_2{\cdot}(CF_3C_6H_5)$

Crystallisation of **8** from α,α,α-trifluorotoluene produces the inclusion compound $(\mathbf{8})_2{\cdot}(CF_3C_6H_5)$ in the orthorhombic space group $P2_12_12_1$. In common with all the subsequent compounds, two independent host molecules (A and B) are present in the asymmetric unit. Unlike these compounds, however, $(\mathbf{8})_2{\cdot}(CF_3C_6H_5)$ crystallises as a conglomerate.[20] This does not result from self-resolution of the two enantiomers of **8** as might have been expected. Individual crystals instead contain only A and B* hosts, or only A* and B hosts, where the asterisk indicates an molecule of **8** with opposite handedness.

Within layers, the pens are generated by screw axes normal to the plane. As for the methylchloroform case, adjacent pens are related by twofold screw axes. Although not required by this combination of symmetry elements, the layers of pens in this structure are not homochiral. Each pen is identical but heterochiral, and has only poor EF interactions at its corners. Adjacent layers of pens are related by twofold screw axes, and so are identical to the first in chiral composition. The pens now have a rhomboid projection (Figure 6) that is more appropriate for the shape of the $CF_3C_6H_5$ guest. As in structure $(\mathbf{8})_2{\cdot}(CH_3CCl_3)$, layers of pens stack offset to each other resulting in the guests becoming enclosed in cages. There are Br···Br interactions both within (3.75 and 3.77 Å) and between (3.69 and 3.80 Å) layers.

The pattern of interlayer C−H···N motifs present in $(\mathbf{8})_2{\cdot}(CH_3CCl_3)$, and shown in Figure 5, part b, arises from A-A*-A-A* etc. host molecule interactions along *b*. In $(\mathbf{8})_2{\cdot}(CF_3C_6H_5)$ the comparable host ordering is A-B*-A-B* etc. (or A*-B-A*-B in an enantiomorphic crystal) along *c*. Hence the general C−H···N arrangement in Figure 5, part b, is repeated for $(\mathbf{8})_2{\cdot}(CF_3C_6H_5)$ since, in both cases, all the interactions occur between opposite **8** enantiomers. They differ in detail, however, due to the presence of the two independent host molecules in $(\mathbf{8})_2{\cdot}(CF_3C_6H_5)$. Consequently, the edge-edge dimer now has C−H···N interac-

Table 2. Some key characteristics of the inclusion compounds formed by host **8** from their crystal structure determinations

Compound of **8** with guest	Weak hydrogen bond motif	C−H···N dimer type	*C*−H···*N* [Å]	C−*H*···*N* [Å]	Angle[a] [°]	Host fold-angle[b] [°]
CH_3CCl_3	double Ar−H···N	edge-edge	3.38	2.47	72.5	97.8
	Ar−H···N···H−CBr−Ar	bifurcated	4.13, 3.78	3.33, 3.09	139.0, 128.0	
$CF_3C_6H_5$	double Ar−H···N	edge-edge	3.52, 3.61	2.62, 2.70	72.0, 71.6	103.7, 104.8
	Ar−H···N···H−CBr−Ar	bifurcated no. 1	4.21, 3.85	3.39, 3.10	140.4, 133.5	
	Ar−H···N···H−CBr−Ar	bifurcated no. 2	4.66, 4.04	3.91, 3.31	133.9, 131.1	
$C_4H_8O_2$	double Ar−H···N	edge-edge	3.59, 3.54	2.61, 2.58	79.1, 77.2	95.8, 99.9
	Ar−H···N···H−CBr−Ar	bifurcated no. 1	3.97, 3.68	3.16, 3.00	139.9, 126.6	
	Ar−H···N···H−CBr−Ar	bifurcated no. 2	3.69, 3.56	2.87, 2.87	140.6, 126.4	
$CHCl_2CHCl_2$	double Ar−H···N	edge-edge	3.51, 3.56	2.54, 2.60	77.0, 75.0	95.7, 99.1
	Ar−H···N···H−CBr−Ar	bifurcated no. 1	3.87, 3.70	3.04, 2.99	141.7, 129.3	
	Ar−H···N···H−CBr−Ar	bifurcated no. 2	3.85, 3.62	3.03, 2.95	140.2, 125.8	
$CHCl_3$	double Ar−H···N	edge-edge	3.47, 3.55	2.51, 2.59	76.8, 77.3	97.5, 101.0
	Ar−H···N···H−CBr−Ar	bifurcated no. 1	3.95, 3.61	3.16, 2.90	138.0, 128.6	
	Ar−H···N···H−CBr−Ar	bifurcated no. 2	3.76, 3.65	2.91, 2.96	142.6, 127.2	
$CH_3CO_2C_2H_5$	double Ar−H···N	edge-edge	3.54, 3.49	2.56, 2.51	78.3, 79.2	97.1, 101.2
	Ar−H···N···H−CBr−Ar	bifurcated no. 1	3.87, 3.59	3.07, 2.90	137.9, 127.2	
	Ar−H···N···H−CBr−Ar	bifurcated no. 2	3.68, 3.69	2.81, 3.00	145.6, 126.7	
CH_3COCH_3	double Ar−H···N	edge-edge	3.56, 3.47	2.59, 2.50	75.4, 78.5	97.4, 101.8
	Ar−H···N···H−CBr−Ar	bifurcated no. 1	3.98, 3.62	3.17, 2.91	138.4, 128.6	
	Ar−H···N···H−CBr−Ar	bifurcated no. 2	3.79, 3.67	2.95, 2.97	142.1, 127.8	
$CHClFCH_2Cl$	double Ar−H···N	edge-edge	3.48, 3.44	2.53, 2.48	74.3, 76.8	97.3, 100.9
	Ar−H···N···H−CBr−Ar	bifurcated no. 1	3.99, 3.55	3.21, 2.84	135.5, 128.4	
	Ar−H···N···H−CBr−Ar	bifurcated no. 2	3.77, 3.73	2.90, 3.03	145.9, 128.4	
C_3H_5CN + CH_3CN	double Ar−H···N	edge-edge	3.56, 3.47	2.60, 2.50	75.6, 77.4	97.2, 100.5
	Ar−H···N···H−CBr−Ar	bifurcated no. 1	4.00, 3.63	3.20, 2.94	138.2, 127.4	
	Ar−H···N···H−CBr−Ar	bifurcated no. 2	3.80, 3.70	2.96, 3.00	142.2, 127.7	

[a] For the double edge-edge Ar-H···N motif, the angle is that between the C···N vector of the intermolecular contact and the normal to the plane of the aryl ring containing this carbon atom. A value of 90° would indicate a perfectly planar array. For the bifurcated Ar−H···N···H−CBr−Ar interaction, the angles are the C−H···N angles. All of these dimer interactions operate between opposite enantiomers of **8**. Hydrogen positions are the calculated values. [b] Host fold-angles are those present between the aromatic wings of host **8** in its pens, and are measured between the three mid bond points illustrated on the structure of **9**.

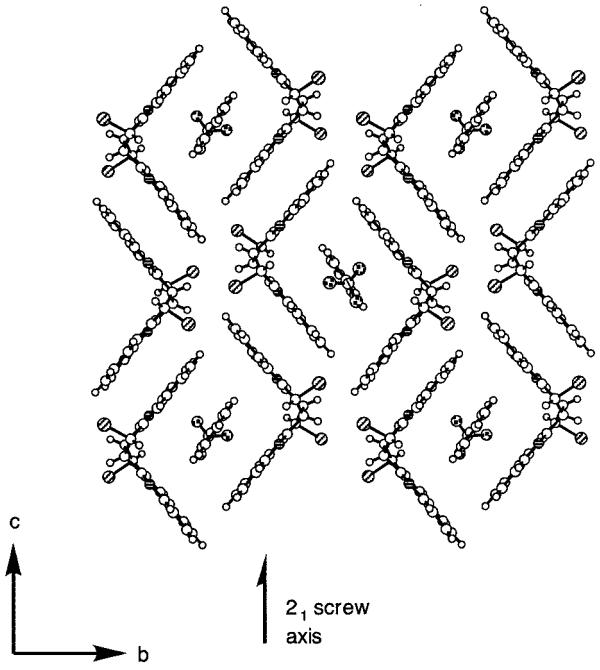

Figure 6. Part of the structure of $(\mathbf{8})_2{\cdot}(CF_3C_6H_5)$ showing a projection in the *bc* plane of one layer of molecular pens and their included guests; fluorine atoms are indicated by stippling

tions of unequal length, and there are two different bifurcated Ar−H···N···H−CBr−Ar arrangements. These individual C−H···N interactions are listed in Table 2.

The Monoclinic $P2_1/c$ Inclusion Compounds of 8

The remaining seven inclusion crystals formed by racemic host **8** with dioxane, 1,1,2,2-tetrachloroethane, chloroform, ethyl acetate, acetone, 1,2-dichlorofluoroethane, and allyl cyanide/acetonitrile, have isostructural host lattices. These crystals, all in the monoclinic space group $P2_1/c$ can, however, have different guest stoichiometry and/or guest packing.

All of these compounds have two independent host molecules (A and B) present in the asymmetric unit, and their structures contain molecular pens with two different geometries but each with an inversion centre at its midpoint. Hence each layer contains only A+A* and B+B* pens.

Adjacent layers stack such that A+A* pens stack over B+B* pens to produce guest-containing channels. In the $P2_1/c$ structures the layers of pens are less well defined than for the first two structures, since the molecules forming the pens are tilted by about 30° out of what would have been the plane layer.

Dioxane, 1,1,2,2-tetrachloroethane, chloroform, and ethyl acetate all yield inclusion compounds with the stoichi-

ometry $(\mathbf{8})_2$·(guest). The first three cases have identical guest arrangements. Compound $(\mathbf{8})_2$·(dioxane) (Figure 7) is described here as a representative example of this subgroup, and details of the chloroform and 1,1,2,2-tetrachloroethane compounds have been deposited.[27]

In structure $(\mathbf{8})_2$·(dioxane) only poor EF interactions operate at the pen corners. There are pairs of Br···Br interactions (3.91 Å) linking molecules of **8** in different channels, and also others (3.90 and 3.91 Å) linking host molecules within a single channel. The adjacent layers of pens are, once again, linked by a network of the two types of double C−H···N interactions. However, the repeat unit has a significantly different hydrogen bonding pattern to that of the earlier inclusion structures (Figure 8, part a). The edge-edge aryl C−H···N dimer still links opposite enantiomers present in adjacent layers, but only between A and A* molecules and by means of a noncentrosymmetric motif (C−*H*···*N* distances 2.61 and 2.58 Å). There is no comparable interaction between the B and B* hosts. In contrast, all the bifurcated dimers operate between A and B molecules of opposite chirality, and it is notable that these C−H···N lengths are considerably shorter than those observed for the first two inclusion structures.

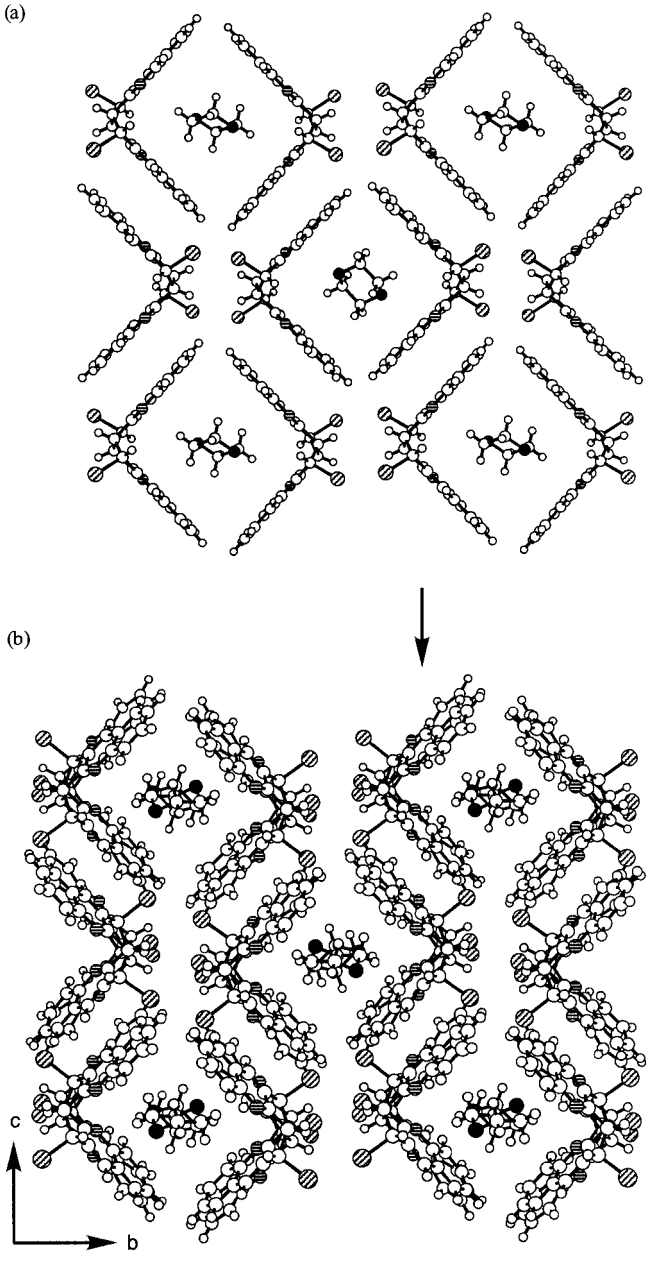

Figure 7. (a) Part of the structure of $(\mathbf{8})_2$·(dioxane) showing a projection in the *bc* plane of one undulating layer of molecular pens and their included guests; the interpen OFF and Br···Br interactions are apparent; A+A* molecules make up the central pen, which is surrounded by four B+B* pens; (b) projection view of two adjacent layers which stack A+A* pens on B+B* pens to produce parallel channels occupied by the dioxane guest molecules; atom designators: N (horizontal hatching), Br (diagonal hatching), O (black); these arrangements should be compared to those in structure $(\mathbf{8})_2$·(CH_3CCl_3) shown in Figure 4

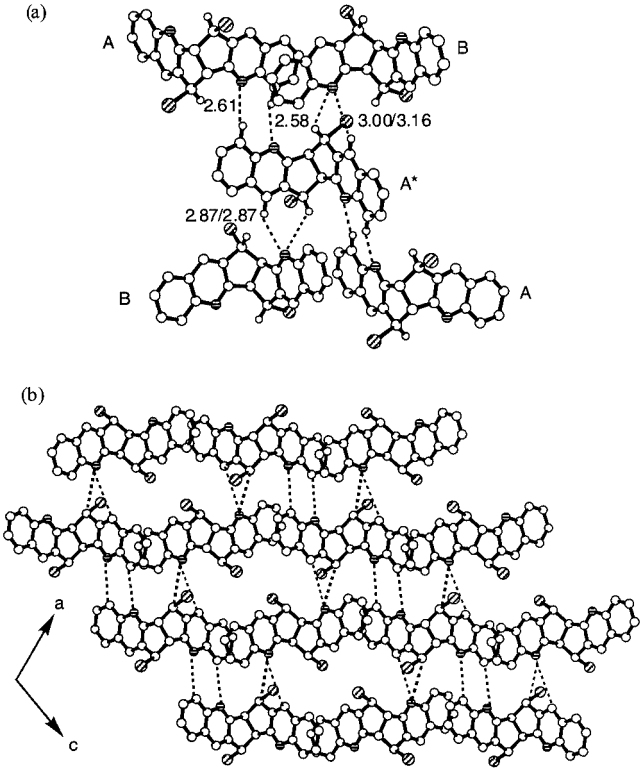

Figure 8. (a) The interlayer double C−H···N weak hydrogen bonds (represented by dashed lines) present in the structure $(\mathbf{8})_2$·(dioxane); each A-type molecule of **8** now subtends four double C−H···N interactions, two of each type, as shown for the central molecule in the diagram; in contrast, each B-type molecule is involved in only two bifurcated dimers; (b) the interlayer C−H···N hydrogen bonding network (dashed lines) between four layers of molecular pens in $(\mathbf{8})_2$·(dioxane); these arrangements should be compared to those for $(\mathbf{8})_2$·(CH_3CCl_3) shown in Figure 5

The interlayer C−H···N network is generated as before by taking four layers (analogous to the two layers shown in Figure 7, part b), selecting a band of molecules of **8** along the *c* axis (indicated by the arrow in Figure 7, part b) that comprises four chains of host molecules of **8**, and then rotating this band into the *ac* plane. The result, shown in Figure 8, part b, reveals part of the interlayer C−H···N hydrogen bonding network.

The pattern of C−H···N weak hydrogen bonding is the same in all seven of the $P2_1/c$ inclusion structures. Indi-

vidual values of the various C−H···N parameters are listed in Table 2.

The location of the guest molecules is one of the principal differences between the two structure types. In $(\mathbf{8})_2\cdot(CH_3CCl_3)$ and $(\mathbf{8})_2\cdot(CF_3C_6H_5)$ each guest occupies a cage, but in the $P2_1/c$ structures the pens stack to produce channels containing the guest molecules. Two different centres of inversion alternate along the channel. These are $a/2$ (about 7.4 Å) apart at $x = 0$ and 0.5 (surrounded by A-A* and B-B* pens, respectively). It is the size and shape of the guest that determines the stoichiometry and arrangement along the channel in the various cases.

With one exception (ethyl acetate), the centre at $x = 0.5$ is always occupied. For the dioxane, 1,1,2,2-tetrachloroethane, and chloroform compounds there is also a guest at, or near, the centre at $x = 0$. This leads to the guest molecules being separated by about 7.4 Å and a stoichiometry of $(\mathbf{8})_2\cdot$(guest).

For the acetone and 1,2-dichlorofluoroethane[27] compounds, there is no guest on the centre at $x = 0$, but rather a pair of centrosymmetrically related guests located on either side of it. This arrangement increases the guest/host ratio to give the stoichiometry $(\mathbf{8})_2\cdot(\text{guest})_{1.5}$. The mixed nitrile guests are also accommodated in this way, with the centre at $x = 0.5$ being occupied by acetonitrile and that at $x = 0$ being surrounded by two allyl cyanide guests to give $(\mathbf{8})_2\cdot(\text{allyl cyanide})_1\cdot(\text{acetonitrile})_{0.5}$.

Finally, in the ethyl acetate compound, the guest is sufficiently large that it is accommodated by having two molecules surrounding the centre at $x = 0$, with the centre at $x = 0.5$ vacant. The stoichiometry returns to $(\mathbf{8})_2\cdot$(guest).

In almost all guest locations discussed above, the guest symmetry cannot comply with the centrosymmetric site symmetry and disorder necessarily occurs. This is usually accompanied by additional positional disorder. Representative examples of guest packing for the $P2_1/c$ structures are illustrated in Figure 9, showing just one disorder component of the guest at each site.

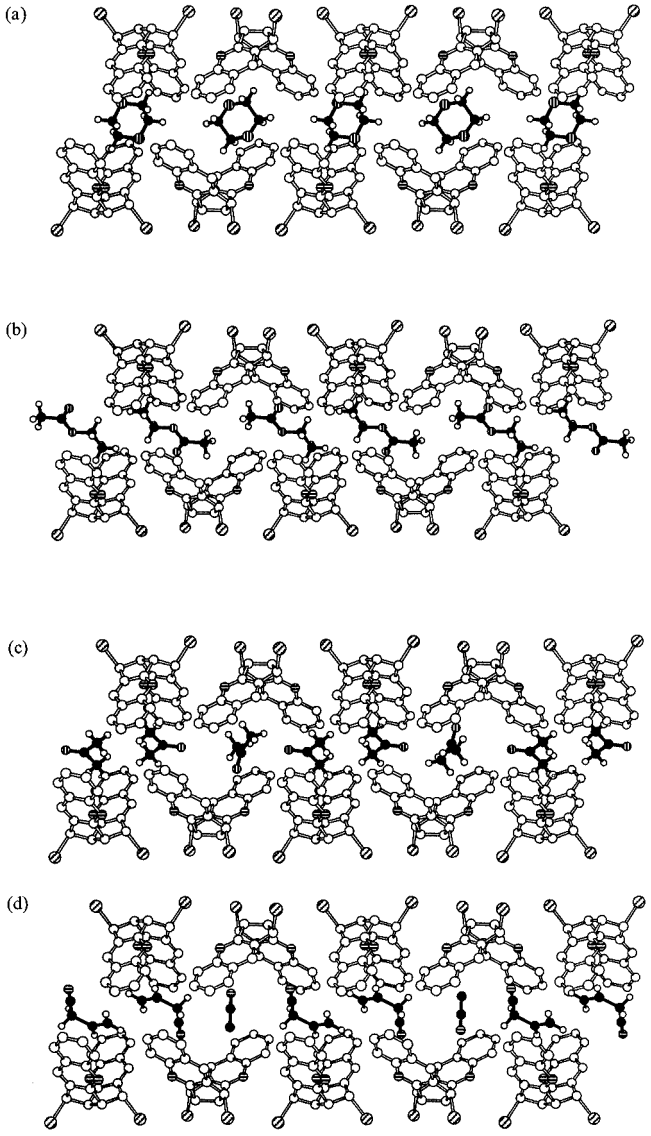

Figure 9. Representative examples of guest packing in one channel of several $P2_1/c$ inclusion compounds; only one guest disorder component is shown at each site; (a) $(\mathbf{8})_2\cdot$(dioxane), (b) $(\mathbf{8})_2\cdot$(ethyl acetate), (c) $(\mathbf{8})\cdot(\text{acetone})_{1.5}$, and (d) $(\mathbf{8})_2\cdot(\text{allyl cyanide})_1\cdot(\text{acetonitrile})_{0.5}$; carbon atoms and bonds are white for the host molecules, and black for the guests

Interactions Between Host and Guests

The two structures with caged guests appear to have been engineered with accommodation of the guest as one of the driving forces. Pens in $(\mathbf{8})_2\cdot(CH_3CCl_3)$ are nearly square and house the guest perfectly, maximising Cl···π aryl interactions which range upwards from 3.5 Å. There are also CH_3···π aryl interactions. In contrast, the pens in $(\mathbf{8})_2\cdot(CF_3C_6H_5)$ are rhomboid, and again are a perfect shape to accommodate the guest. This is located within the pen so that it is parallel to two opposite pen walls and normal to the other two. This leads to favourable OFF and EF interactions. The CF_3 group does not interact with the pen walls, but there is F···Br contact between layers.

In the remaining structures, the guest is housed within a channel, so various favourable interactions are possible, depending on the nature of the guest. Where the guest contains chloro atoms, the guest orientation maximises Cl···π aryl interactions. Those guests that are planar (or have planar portions) are aligned with the pen walls, again leading to maximum interaction with the host aryl wings. Guests with oxygen-containing functional groups participate in C−H···O interactions.

Host Ring-Folding

A measure of the molecular folding of **8** in the various compounds is provided by the host fold-angle, defined as the angle between the three bond centroids marked on the molecular structure **9**.

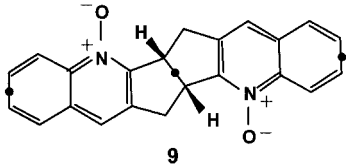

9

The shapes of the **8** pens can be square, rhomboid, or rectangular, in projected cross-section. However, the range of fold-angles observed is very restricted with all seventeen values lying between 95.7 and 104.8° (see Table 2). The values for the compounds with isostructural host lattices have ranges of just 95.7−97.5° for the A+A* pens, and 99.1−101.8° for the B+B* pens. The single value (97.8°) observed for $(\mathbf{8})_2\cdot(CH_3CCl_3)$ lies between these, but both values for $(\mathbf{8})_2\cdot(CF_3C_6H_5)$ are bigger.

Since the central bicyclo[3.3.0]octane ring is flexible, there is no fundamental barrier to different fold-angles being adopted in related diquinoline molecules. For example, the value observed for the parent compound **7** is greater (107.3°), and that of its bis(*N*-oxide) derivative **9**[28] is considerably greater (141.4°).

Conclusions

The behaviour of diquinoline **8** fully confirmed our planned design of a new lattice inclusion host. It traps a wide range of small organic guest molecules but, despite considerable effort, we were unable to obtain the crystalline guest-free substance. The structural consistency of the inclusion compounds formed by **8** is remarkable. In all cases, pairs of host molecules enclose the guest by forming quadrilateral molecular pens that then pack into layers. Indeed, seven of the nine compounds investigated have an isostructural host lattice.

The similarity of these inclusion compounds is in marked contrast to the variety of structural types observed earlier for the homologue **3**. Host **3** prefers to adopt different lattices to accommodate its strong preference for small polyhalogenated guests,[8] whereas host **8** prefers the same type of host lattice but is catholic in the types of guest it includes. Although both hosts potentially can employ the same types of weak intermolecular forces, their supramolecular behaviour in fact proves to be very different. The only molecular difference between these two host molecules is a CH_2 group in the central linker group.

Although the central linker in **8** is flexible, there is a remarkable consistency in fold-angles throughout the inclusion compounds of **8**. We ascribe this, and the effective nature of **8** as a host, to the dominance of two major supramolecular synthons. The well-known aromatic OFF interaction allows the molecules to assemble into layers of pens, while the less-known C−H···N interaction cements these layers together. Two different types of double C−H···N motifs operate in this manner. As we have observed in other work,[7b] the higher order double C−H···N interactions represent much more useful and robust motifs for crystal engineering than the simpler single interaction.

Experimental Section

General: ^{1}H (300 MHz) and ^{13}C (75 MHz) NMR spectra were recorded with a Bruker ACF300 instrument at 25 °C and are reported as chemical shifts (δ) relative to TMS. The substitution of carbon atoms was determined by the DEPT procedure. Melting points were determined with a Kofler instrument and are uncorrected. IR spectra were recorded with a Perkin−Elmer 298 infrared spectrophotometer. Routine mass spectra (EI) were recorded with a VG Quattro triple quadrupole instrument by Dr. J. J. Brophy. Elemental analyses (C,H,N and HRMS) were carried out at The Australian National University in Canberra.

5bα,6,12bα,13-Tetrahydropentaleno[1,2-*b*:4,5-*b*′]diquinoline (7): 2-Aminobenzaldehyde[16] (**5**) (3.54 g, 2.90 mmol) and bicyclo[3.3.0]-octane-2,6-dione[17] (**6**) (1.38 g, 10.0 mmol) were dissolved with stirring in methanol (15.0 mL) and the mixture cooled to 0 °C. Aqueous NaOH (2.00 M, 2.50 mL) then was added dropwise. The mixture was allowed to warm to room temperature as it was stirred overnight. The crude solid product was filtered, triturated with a small volume of ethyl acetate, and then refiltered to give the diquinoline **7** (2.30 g, 75%). M.p. 272.0−272.5 °C (from ethanol). ^{1}H NMR ($CDCl_3$): δ = 3.70 and 3.76 (both d, $^2J_{AB}$ = 17.0, ^3J = 6.8 Hz, 2 H), 3.86 and 3.91 (both s, $^2J_{AB}$ = 17.0 Hz, 2 H), 4.32 (d, ^3J = 6.8 Hz, 2 H), 7.39−7.44 (m, 2 H), 7.58−7.69 (m, 4 H), 7.89 (s, 2 H), 8.07 (d, ^3J = 8.3 Hz, 2 H) ppm. ^{13}C NMR ($CDCl_3$): δ = 35.2 (CH_2), 47.7 (CH), 126.0 (CH), 127.5 (CH), 127.7 (CH), 128.0 (C), 128.9 (CH), 132.1 (CH), 134.5 (C) 147.4 (C), 167.6 (C) ppm. IR (paraffin mull): $\tilde{\nu}$ = 1600 w, 1560 w, 1405 w, 1295 w, 1215 w, 1140 w, 940 w, 855 w, 745 w cm^{-1}. MS: *m*/*z* (> 10%) = 309 (25), 308 (100) [M$^+$], 307 (80), 306 (25), 305 (27), 281 (20), 180 (11), 154 (10), 153 (13), 140 (10). $C_{22}H_{16}N_2$ (308.4): calcd. C 85.69, H 5.23, N 9.08; found C 85.60, H 5.20, N 9.13.

6α,13α-Dibromo-5bα,6,12bα,13-tetrahydropentaleno[1,2-*b*:4,5-*b*′]-diquinoline (8): A solution of diquinoline **7** (1.02 g, 3.30 mmol) and *N*-bromosuccinimide (NBS) (1.78 g, 10.0 mmol) was stirred and refluxed overnight in CCl_4 (150 mL). The mixture was allowed to cool and succinimide removed by filtration. This solid was washed with CCl_4, and the solvent evaporated from the filtrate under reduced pressure to yield the rather labile crude product. This was purified by elution through a column of silica using CH_2Cl_2 as eluent to give the dibromide **8** (1.20 g, 78%). M.p. 135−137 °C (dec.). ^{1}H NMR ($CDCl_3$): δ = 4.89 (s, 2 H), 6.42 (s, 2 H), 7.49−7.54 (m, 2 H), 7.70−7.78 (m, 4 H), 8.18−8.23 (m, 4 H) ppm. ^{13}C NMR ($CDCl_3$): δ = 48.5 (CH), 57.6 (CH), 127.3 (CH), 128.0 (CH), 128.3 (CH), 131.0 (CH), 134.9 (C), 135.2 (CH), 147.6 (C), 161.5 (C) ppm, plus one signal of aromatic C obscured. IR (paraffin mull): $\tilde{\nu}$ = 1595 m, 1400 w, 1255 w, 1200 w, 1140 m, 780 w, 745m cm^{-1}. MS: *m*/*z* (> 15%) = 468 (3) [M$^+$, 2 ^{81}Br], 466 (6) [M$^+$, ^{79}Br/^{81}Br], 464 (3) [M$^+$, 2 ^{79}Br], 387 (35), 385 (35), 307 (40), 306 (93), 305 (86), 304 (24), 303 (20), 153 (100), 152 (47), 139 (24), 138 (17). HRMS: *m*/*z* calcd. for $C_{22}H_{14}Br_2N_2^+$ [M$^+$] 467.948279, 465.950325, 463.952371; found 467.948993, 465.951570, 463.953220. Crystals of the individual inclusion compounds were grown by slow concentration of solutions of **8** in the relevant solvent.

Determination of the Crystal Structures: For all structures, reflection data were measured with an Enraf−Nonius CAD-4 diffractometer in the θ/2θ scan mode using graphite-monochromated molybdenum radiation (λ = 0.7107 Å), except those of **7** and $(\mathbf{8})_2$·(chloroform) where copper radiation (λ = 1.5418 Å) was used instead. Data were corrected for absorption[29] except for **7**. Reflections with $I > 2\sigma(I)$ were considered observed. The structures were determined by direct phasing (SIR92[30]) and Fourier methods. Hydrogen atoms for each structure were included in calculated positions. The non-hydrogen atoms of each host molecule were refined with independent positional parameters. Refinement of **7** was anisotropic for all non-hydrogen atoms. For the host molecules in the remaining structures, individual anisotropic temper-

ature parameters were assigned to the bromine atoms, and a 15-parameter TLX rigid-body thermal parameter (where T is the translation tensor, L is the libration tensor and X is the origin of libration) described the thermal motion of the remaining atoms.[31] Guest modelling varied for the different structures. In most, the guests were located at, or near, centres of inversion and so were disordered. Some exhibited positional disorder also. For refinement, all guests were modelled as rigid groups and were assigned TLX thermal parameters. Reflection weights used were $1/\sigma^2(F_o)$, with $\sigma(F_o)$ being derived from $\sigma(I_o) = [\sigma^2(I_o) + (0.04I_o)^2]^{1/2}$. The weighted residual was defined as $R_w = (\Sigma w\Delta^2/\Sigma wF_o^2)^{1/2}$. Atomic scattering factors and anomalous dispersion parameters were from the International Tables for X-ray Crystallography.[32] CCDC-189724 to -189733 (see individual compound listings in Table 1 and ref.[27]) contain the supplementary crystallographic data for this paper. These data can be obtained free of charge at www.ccdc.cam.ac.uk/conts/retrieving.html or from the Cambridge Crystallographic Data Centre, 12 Union Road, Cambridge CB2 1EZ, UK [Fax: (internat.) + 44-1223/336-033; E-mail: deposit@ccdc.cam.ac.uk].

Acknowledgments

We gratefully thank the Australian Research Council for financial support of this work.

[1] *Inclusion Compounds* (Eds.: J. L. Atwood, J. E. D. Davies, D. D. MacNicol), Academic Press, London, **1984**, vol. 1−3; Oxford University Press, Oxford, **1991**, vol. 4−5.
[2] *Comprehensive Supramolecular Chemistry*, vol. 1−11 (Eds.: J. L. Atwood, J. E. D. Davies, D. D. MacNicol, F. Vögtle), Pergamon, Oxford, **1996**.
[3] J.-M. Lehn, *Angew. Chem. Int. Ed. Engl.* **1990**, *29*, 1304−1319; *Angew. Chem.* **1990**, *102*, 1347−1362.
[4] [4a] M. C. Etter, *Acc. Chem. Res.* **1990**, *23*, 120−126. [4b] M. C. Etter, *J. Phys. Chem.* **1991**, *95*, 4601−4610. [4c] G. R. Desiraju, T. Steiner, *The Weak Hydrogen Bond in Structural Chemistry and Biology*, Oxford University Press, Oxford, **1999**.
[5] [5a] G. R. Desiraju, *Angew. Chem. Int. Ed. Engl.* **1995**, *34*, 2311−2327; *Angew. Chem.* **1995**, *107*, 2541−2558. [5b] *The Crystal as a Supramolecular Entity* (Ed.: G. R. Desiraju), Wiley, New York, **1996**.
[6] [6a] G. R. Desiraju, *Crystal Engineering: The Design of Molecular Solids*, Elsevier, Amsterdam, **1989**. [6b]Y.-L. Chang, M.-A. West, F. W. Fowler, J. W. Lauher, *J. Am. Chem. Soc.* **1993**, *115*, 5991−6000. [6c] C. B. Aakeröy, K. R. Seddon, *Chem. Soc. Rev.* **1993**, *22*, 397−407. [6d] C. B. Aakeröy, *Acta Crystallogr., Sect. B* **1997**, *53*, 569−586.
[7] [7a] C. E. Marjo, R. Bishop, D. C. Craig, M. L. Scudder, *Aust. J. Chem.* **1996**, *49*, 337−342. [7b] C. E. Marjo, R. Bishop, D. C. Craig, M. L. Scudder, *Eur. J. Org. Chem.* **2001**, 863−873.
[8] C. E. Marjo, R. Bishop, D. C. Craig, A. O'Brien, M. L. Scudder, *J. Chem. Soc., Chem. Commun.* **1994**, 2513−2514.
[9] [9a] C. E. Marjo, M. L. Scudder, D. C. Craig, R. Bishop, *J. Chem. Soc., Perkin Trans. 2* **1997**, 2099−2104. [9b] R. Bishop, C. E. Marjo, M. L. Scudder, *Mol. Cryst. Liq. Cryst.* **1998**, *313*, 75−83.
[10] R. W. Hoffman, *Angew. Chem. Int. Ed. Engl.* **1992**, *31*, 1124−1134, *Angew. Chem.* **1992**, *104*, 1147−1157.
[11] [11a] G. R. L. Cousins, S.-A. Poulsen, J. K. M. Sanders, *Curr. Opin. Chem. Biol.* **2000**, *4*, 270−279. [11b] P. S. Lukeman, J. K. M. Sanders, *Tetrahedron Lett.* **2000**, *41*, 10171−10174.
[12] R. Bishop, in *Comprehensive Supramolecular Chemistry*, vol. 6 (Eds.: D. D. MacNicol, F. Toda, R. Bishop), Pergamon, Oxford, **1996**, chapter 4, pp. 85−115.
[13] [13a] R. Taylor, O. Kennard, *J. Am. Chem. Soc.* **1982**, *104*, 5063−5070. [13b] D. S. Reddy, B. S. Goud, K. Panneerselvam, G. R. Desiraju, *J. Chem. Soc., Chem. Commun.* **1994**, 663−664. [13c] R. S. Rowland, R. Taylor, *J. Phys. Chem.* **1996**, *100*, 7384−7391. [13d] C. Foces−Foces, N. Jagerovic, J. Elguero, *Acta Crystallogr., Sect. C* **2000**, *56*, 215−218.
[14] For discussion and a comprehensive review of C−H···N and other weak hydrogen bonding motifs, see: G. R. Desiraju, T. Steiner, *The Weak Hydrogen Bond in Structural Chemistry and Biology*, Oxford Science Publications, Oxford, **1999**, in particular chapter 2, pp. 29−121 and chapter 4, pp. 293−342.
[15] [15a] G. R. Desiraju, *Acc. Chem. Res.* **1996**, *29*, 441−449. [15b] A. Gavezzotti, *Cryst. Rev.* **1998**, *7*, 5−121.
[16] L. I. Smith, J. W. Opie, *Org. Synth., Coll. Vol.* **1955**, *III*, 56−58.
[17] A. A. Hagedorn III, D. G. Farnum, *J. Org. Chem.* **1977**, *42*, 3765−3767.
[18] [18a] C.-C. Cheng, S. J. Yang, *Org. React.* **1982**, *28*, 37−201. [18b] R. P. Thummel, *Synlett* **1992**, 1−12.
[19] J. Jacques, A. Collet, S. H. Wilen, *Enantiomers, Racemates, and Resolutions*, Wiley, New York, **1981**.
[20] [20a] A. Collet, M.-J. Brienne, J. Jacques, *Chem. Rev.* **1980**, *80*, 215−230. [20b] A. Collet, "The Homochiral versus Heterochiral Packing Dilemma", in *Problems and Wonders of Chiral Molecules* (Ed.: M. Simonyi), Akadémiai Kiadó, Budapest, **1990**, pp. 91−109.
[21] C. A. Hunter, K. R. Lawson, J. Perkins, C. J. Urch, *J. Chem. Soc., Perkin Trans. 2* **2001**, 651−669.
[22] H. Suezawa, T. Yoshida, M. Hirota, H. Takahashi, Y. Umezawa, K. Honda, S. Tsuboyama, M. Nishio, *J. Chem. Soc., Perkin Trans. 2* **2001**, 2053−2058.
[23] A preliminary account of the 1,1,1-trichloroethane and chloroform compounds (CSD refcodes LICGIN and LICHIO) has been published: A. N. M. M. Rahman, R. Bishop, D. C. Craig, M. L. Scudder, *Chem. Commun.* **1999**, 2389−2390.
[24] [24a] F. Diederich, *Cyclophanes: Monographs in Supramolecular Chemistry*, The Royal Society of Chemistry, Cambridge, **1991**, vol. 2. [24b] F. Vögtle, *Cyclophane Chemistry*, Wiley, Chichester, **1993**.
[25] [25a] J. A. R. P. Sarma, G. R. Desiraju, *Acc. Chem. Res.* **1986**, *19*, 222−228. [25b] O. Navon, J. Bernstein, V. Khodorovsky, *Angew. Chem. Int. Ed. Engl.* **1997**, *36*, 601−603, *Angew. Chem.* **1997**, *109*, 640−642.
[26] S. F. Alshahateet, R. Bishop, D. C. Craig, M. L. Scudder, *CrystEngComm* **2001**, *3(55)*, 264−269.
[27] Crystal data:
(**8**)$_2$·(chloroform): $(C_{22}H_{14}Br_2N_2)_2$·$(CHCl_3)$, M = 1051.8, $P2_1/c$, a = 14.832(7), b = 16.754(5), c = 18.084(9) Å, β = 110.80(2)°, V = 4201(3) Å^3, Z = 4, μ(Cu-K$_\alpha$) = 6.823 mm^{-1}, R = 0.052, R_w = 0.079 for 4680 observed reflections (CCDC-189731).
(**8**)$_2$·(1,1,2,2-tetrachloroethane): $(C_{22}H_{14}Br_2N_2)_2$·$(C_2H_2Cl_4)$, M = 1100.2, $P2_1/c$, a = 14.866(7), b = 17.135(7), c = 17.845(8) Å, β = 110.69(3) °, V = 4252(3) Å^3, Z = 4, μ(Mo-K_α) = 4.040 mm^{-1}, R = 0.052, R_w = 0.073 for 3049 observed reflections (CCDC-189732).
(**8**)$_2$·(1,2-dichlorofluoroethane)$_{1.5}$: $(C_{22}H_{14}Br_2N_2)_2$·$(C_2H_3Cl_2F)_{1.5}$, M = 1107.8, $P2_1/c$, a = 14.945(7), b = 16.913(8), c = 18.057(8) Å, β = 111.04(3) °, V = 4260(3) Å^3, Z = 4, μ(Mo-K_α) = 3.977 mm^{-1}, R = 0.073, R_w = 0.094 for 2493 observed reflections (CCDC-189733).
[28] V. T. Nguyen, A. N. M. M. Rahman, R. Bishop, D. C. Craig, M. L. Scudder, *Aust. J. Chem.* **1999**, *52*, 1047−1053.
[29] J. De Meulenaer, M. Tompa, *Acta Crystallogr.* **1965**, *19*, 1014−1018.
[30] A. Altomare, G. Cascarano, C. Giacovazzo, A. Guagliardi, M. C. Burla, G. Polidori, M. Camalli, *J. Appl. Crystallogr.* **1994**, *27*, 435.
[31] A. D. Rae, *RAELS − A Comprehensive Constrained Least Squares Refinement Program*, University of New South Wales, **1989**.
[32] *International Tables for X-ray Crystallography*, vol. 4 (Eds.: J. A. Ibers, W. C. Hamilton), Kynoch Press, Birmingham, **1974**.

Received July 19, 2002
[O02402]